Model Predictive Control of a Current Source Inverter together with its Current Source

Pablo Cossutta
Mathias Angelico Engelhardt
and Miguel Pablo Aguirre
CIDEI - Instituto Tecnológico de Buenos Aires
Buenos Aires, Argentina
pcossutt@itba.edu.ar

Marco Rivera
Department of Industrial Technologies
Universidad de Talca
Curicó, Chile
marcoriv@utalca.cl

María Inés Valla
LEICI - UNLP
Universidad Nacional de La Plata
La Plata, Argentina
m.i.valla@ieee.org

***Abstract*—Over the past years a great amount of research has been done to interconnect different energy sources with the power grid or different types of loads. Current source inverters have proved to be a good option due to its high reliability, fault tolerant capabilities, quasi soft switching and the use of lower capacitor values among others. Most of the current source inverters topologies have a current source as input, which could be implemented with a buck converter, and they are controlled with cascaded linear control (usually PI controller), rotating frame coordinate transformation and a modulation stage. In this paper a predictive control strategy of a current source inverter together with its associated current source is presented. This strategy allows to track not only the output voltages at the load but also the current source within a single controller. The control algorithm makes use of a discrete time model of the whole system so as to predict its future behaviour for each one of the available switching combinations. Each one of the predicted values are used to minimize a set of predefined control goals within a multiple term cost function that includes cost associated with the commutation frequency and the reference tracking. Simulation results show a good behaviour and fast dynamics with a low switching frequency of all the switches involved. These characteristics make the proposed controller a suitable option to use with high power inverters.**

I. INTRODUCTION

The need for efficient ways to interconnect energy sources with either the power grid or different types of loads has increased the amount of research carried out in power electronics converters. Current source inverters (CSI) and multilevel current source inverters (MCSI) have been proved to be a good option due to their low harmonic distortion, efficiency and fault tolerance when used in motor applications [1], [2] and to drive energy sources such as wind farms, fuel cells and photovoltaic [3]–[5]. The CSI is traditionally controlled with classic cascaded linear control loops (usually PI controllers), rotating frame coordinate transformations and a modulation stage [6]–[8]. A new kind of controllers based on finite control set model predictive control (FCS - MPC) has been found in the literature [9]. FCS-MPC has been introduced for matrix converters [10], [11], active front ends [12], [13], for single and multilevel inverters [14]–[17] and to improve the dynamic performance of a converter [18], among other applications. This kind of controllers are inherently suitable for limited number of switching states of power converters [19]. A discrete time model of the CSI is used to predict the future values of the state variables for each one of the switching state. These predicted values are used to evaluate a cost function in order to achieve a good reference tracking, to operate at a low switching frequency and reduce the total harmonic distortion. The control strategy is performed by generating the switching state that minimizes the cost function and better meets the control goals. The prediction horizon could be increased in order to achieve a better performance, taking into account that this is limited by the model accuracy and the computational power of the implementation. The CSI topology is fed by a current source that could be implemented by a buck converter driven by a renewable energy sources such as fuel cells, solar panels or wind generators [8]. These kind of sources could suffer non continuous changes in the voltage output therefore the buck converter has to be controlled to deliver the right amount of energy to the CSI.

In this paper the predictive control of the CSI is presented with the switch state of the buck converter as part of the predictive control strategy. A complete model of both converters is used to control not only the output voltage of the CSI but also its input current, reducing the switching frequency and therefore the harmonic distortion of the overall system.

II. OVERALL SYSTEM MODEL

A. Topology

Fig. 1 shows the entire system. It is composed of a voltage source, a current buck converter and a typical CSI converter. The CSI has six reverse blocking switches that could be implemented with either insulated gate bipolar transistors (IGBT) each one with a series diode to block the reverse current or integrated gate commutated thyristors (IGCT) [20]. A three phase capacitor is placed at the output to filter the harmonic distortion produced by the commutation of the switches and to improve both current and voltage waveforms of the load. Filter capacitors in Fig. 1 are placed in star configuration as in the mathematical model. They could also be connected in delta configuration where the capacitance value gets reduced to one third and the voltage rating is increased by a factor of $\sqrt{3}$. The input current of the CSI is delivered

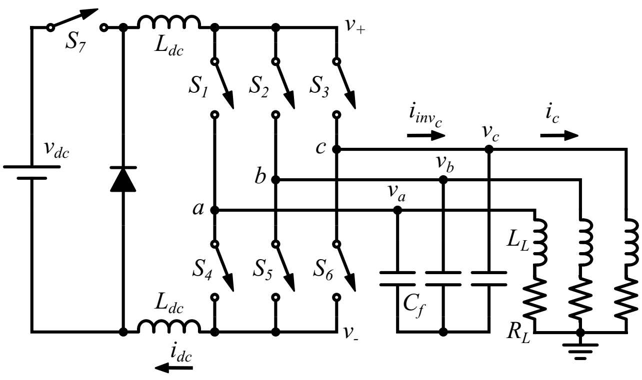

Fig. 1. Topology

by the buck converter which is connected to a voltage source.

B. Mathematical Model of the System

The predictive control strategy requires a mathematical model of the entire plant to calculate a prediction of the values of interest for each switch state of the CSI and the buck converter. At any given time, the CSI must grant a current path so one upper switch and one lower switch must be conducting. Furthermore, only one of the upper and lower devices can be conducting in order to ensure the current injected by the inverter is well known and the output current waveform is defined. These restrictions can be stated as follows

$$S_1 + S_2 + S_3 = S_4 + S_5 + S_6 = 1 \tag{1}$$

Therefore, the first step is to define how many switching states the system has. This CSI topology has nine possible states as presented in Table I. i_a, i_b and i_c are the output currents of the inverter, and v_{csi} is the voltage difference at the input terminals of the inverter v_+ and v_-. Taking into account that the proposed topology has one extra switch due to the buck converter, the system doubles the number of states to analyze. The voltage v_{csi} can be determined by the switching states and the voltage at the output capacitors v_a, v_b and v_c. Its expression is

$$v_{csi} = (S_1 - S_4)v_a + (S_2 - S_5)v_b + (S_3 - S_6)v_c \tag{2}$$

Equation (3) shows the relationship between the output current of the buck converter i_{dc}, the state of its switch S_7 and the input voltage of the CSI v_{csi}, where $2\,L_{dc}$ is the inductance of the buck converter and v_{dc} is the input voltage source.

$$\frac{\mathrm{d}}{\mathrm{d}t} i_{dc} = \frac{v_{dc}}{2\,L_{dc}} S_7 - \frac{v_{csi}}{2\,L_{dc}} \tag{3}$$

Then, the current injected by the inverter can be defined according to the switching signals and the output current of the buck converter.

$$i_{inv_a} = (S_1 - S_4)\, i_{dc} \tag{4a}$$
$$i_{inv_b} = (S_2 - S_5)\, i_{dc} \tag{4b}$$
$$i_{inv_c} = (S_3 - S_6)\, i_{dc} \tag{4c}$$

Finally, the dynamic model of the load and filter capacitors are taken into account within the model,

$$\begin{cases} \dfrac{d}{dt} v_x = \dfrac{i_{inv\,x} - i_x}{C_f} \\ \dfrac{d}{dt} i_x = \dfrac{v_x - R_L\, i_x}{L_L} \end{cases} \quad with\, x : \{a, b, c\} \tag{5}$$

where C_f is the filter capacitance, L_L is the load inductance and R_L is the load resistance.

TABLE I
OUTPUT CURRENT AND VOLTAGE AT THE INPUT OF THE CSI AT EACH STATE

State	S_1	S_2	S_3	S_4	S_5	S_6	i_a	i_b	i_c	v_{csi}
#1	1	0	0	1	0	0	0	0	0	0
#2	1	0	0	0	1	0	i_{dc}	-i_{dc}	0	v_{ab}
#3	1	0	0	0	0	1	i_{dc}	0	-i_{dc}	v_{ac}
#4	0	1	0	1	0	0	-i_{dc}	i_{dc}	0	v_{ba}
#5	0	1	0	0	1	0	0	0	0	0
#6	0	1	0	0	0	1	0	i_{dc}	-i_{dc}	v_{bc}
#7	0	0	1	1	0	0	-i_{dc}	0	i_{dc}	v_{ca}
#8	0	0	1	0	1	0	0	-i_{dc}	i_{dc}	v_{cb}
#9	0	0	1	0	0	1	0	0	0	0

III. Model Predictive Control Strategy

The proposed predictive strategy found in the literature [21] uses the discrete model of the system to make a prediction of the following state variables for each one of the switching states, shown in Table I, and the switching state of the buck converter. The controller uses the available switching states to obtain the best control action that meets some control goals predefined within the cost function. Detailed descriptions of the prediction model and the cost function optimization are presented in the following subsections.

A. Prediction Model

The core of the controller is the prediction model and taking into consideration that the algorithm is implemented on digital platforms, a discrete time approximation of the system model needs to be calculated. The Euler forward approximation for the derivative is used in this paper because the sampling period is smaller than the dynamics of the system. After discretization the model equations can be packed together to obtain the discrete space state representation.

$$\begin{bmatrix} v_a \\ v_b \\ v_c \\ i_a \\ i_b \\ i_c \end{bmatrix}_{k+1} = \begin{bmatrix} 1 & 0 & 0 & a & 0 & 0 \\ 0 & 1 & 0 & 0 & a & 0 \\ 0 & 0 & 1 & 0 & 0 & a \\ b & 0 & 0 & c & 0 & 0 \\ 0 & b & 0 & 0 & c & 0 \\ 0 & 0 & b & 0 & 0 & c \end{bmatrix} \begin{bmatrix} v_a \\ v_b \\ v_c \\ i_a \\ i_b \\ i_c \end{bmatrix}_k - a \begin{bmatrix} S_1 - S_4 \\ S_2 - S_5 \\ S_3 - S_6 \\ 0 \\ 0 \\ 0 \end{bmatrix}_k i_{dc_k} \tag{6}$$

$$a = -\frac{T_s}{C_f} \qquad b = \frac{T_s}{L_L} \qquad c = 1 - b\, R_L \tag{7}$$

The state variables of the CSI are the filter capacitor voltages v_{a_k}, v_{b_k}, v_{c_k}, the currents of the load i_{a_k}, i_{b_k} and i_{c_k} . The input of the model are the state of the switches. Since the capacitor voltages depend on the output current of the buck converter, a new set of equations are presented to describe the behaviour of the buck converter.

$$v_{csi_k} = (S_{1_k} - S_{4_k})v_{a_k} + (S_{2_k} - S_{5_k})v_{b_k} + (S_{3_k} - S_{6_k})v_{c_k} \quad (8)$$

$$i_{dc_{k+1}} = i_{dc_k} + \frac{T_s}{2L_{dc}} \begin{bmatrix} -1 & V_{dc} \end{bmatrix} \begin{bmatrix} v_{csi_k} \\ S_{7_k} \end{bmatrix} \quad (9)$$

As shown in (6) the output voltages of the CSI change one sample time after a change on its switches (S_{1-6}) is applied. From (9), it can be seen that the current of the buck converter changes one sample time after its switch (S_7) commutates. At instant k a new set of measurements are taken and the proposed algorithm uses the model to predict the output voltage in the filter capacitors and output current of the buck at $k+2$ applying (6) and (9) two times. In order to take into account the calculation delay, it is considered that the chosen switching state is applied at $k+1$. As there are 9 states for the CSI and 2 states for the buck converter, the controller takes into consideration a total of 18 possible states in each prediction sample to minimize the cost function.

B. Cost Function Optimization

After all the prediction values at the instant $k+2$ are obtained, they are used to evaluate a cost function that deals with different control goals. The primary term of the cost function, related to the CSI switching states, is defined by the sum of the squared tracking errors:

$$\begin{aligned} c_{v_{ref}} = (v_{a_{k+2}} - v^*_{a_{k+2}})^2 + (v_{b_{k+2}} - v^*_{b_{k+2}})^2 \\ + (v_{c_{k+2}} - v^*_{c_{k+2}})^2 \end{aligned} \quad (10)$$

Regarding the buck converter the reference is a constant predefined current and the cost function term is stated as:

$$c_{i_{dc}} = (i_{dc_{k+2}} - i_{dc_{ref}})^2 \quad (11)$$

The future capacitor voltage reference is defined at instant $k+1$ can be estimated using fourth order Lagrange extrapolation given by

$$v^*_{k+1} = 4v^*_k - 6v^*_{k-1} + 4v^*_{k-2} - v^*_{k-3} \quad (12)$$

Thus it can be extrapolated to predict the reference at the next sample period by

$$v^*_{k+2} = 10v^*_k - 20v^*_{k-1} + 15v^*_{k-2} - 4v^*_{k-3} \quad (13)$$

According to the literature this estimation can be used for a wide range of frequencies of v^* [22]. If the sampling time is sufficiently small no extrapolation is required since the reference signal is a sine wave at line frequency. The predictive strategy allows the addition of other constraints within the cost function [19]. In this kind of systems it is desired to reduce the switching frequency, reducing power losses in the switches during their commutation and hence increasing the overall efficiency. In order to add this constraint a new term is added to the cost function. This term penalizes the switching state transitions that produce the largest number of changes in the switches from one sampling period to the next.

The following equation is used to calculate the number of commutations in the CSI that occurs at every sampling instant.

$$N_{comm} = \sum_{i=1}^{6} \left| S_{i_{k+1}} - S_{i_k} \right| \quad (14)$$

The penalization terms for both the switches of the CSI and the buck converter are given by

$$c_{comm} = \lambda_{csi} N_{comm} + \lambda_{buck} \left| S_{7_{k+1}} - S_{7_k} \right| \quad (15)$$

In order to normalize all the cost function terms each of them are weighted by a factor defined by

$$\lambda_{vref} = \frac{1}{e^2_{vref}} \qquad \lambda_{i_{dc}} = \frac{1}{e^2_{i_{dc}}} \quad (16)$$

e_{vref} and $e_{i_{dc}}$ are the error limits of the output voltage and buck current, respectively. Finally, the sum of the terms weighted by their factors leads to the global cost function that is

$$\begin{aligned} c_{global} = \lambda_{v_{ref}} c_{v_{ref}} + \lambda_{i_{dc}} c_{i_{dc}} + \lambda_{csi} N_{comm} \\ + \lambda_{buck} \left| S_{7_{k+1}} - S_{7_k} \right| \end{aligned} \quad (17)$$

After all the calculations were performed, the switching state that minimize the global cost function (17), is chosen and applied at the instant $k+1$.

IV. Simulation Results

The proposed control method is validated through a simulation carried out using MATLAB/Simulink with a model of a CSI with the parameters indicated in Table II. The prediction is done with a sampling time equal to Ts. The weighting factors are chosen after several simulations to obtain optimal results.

In the following subsections the system behaviour is tested under nominal conditions and a step down change of the external output voltage reference and the external input current reference. Although is not shown in this paper, similar results are found when a step up test is performed in both references.

TABLE II
System parameters

Symbol	Definition	Value
v_{dc}	Voltage source	5kV
R_{load}	Load resistor	15Ω
L_{load}	Load inductor	6mH
L_{dc}	DC inductor	120mH
C_f	Filter capacitors (Δ)	22.2μF
T_s	Sampling time	200μs
f_l	Reference frequency	50Hz
$i_{dc_{ref}}$	Reference current	200A
v_{ref}	Reference voltage	2.9kV
e_{vref}	Acceptable voltage error	0.01 v_{ref}
$e_{i_{dc}}$	Acceptable current error	0.01 $i_{dc_{ref}}$
λ_{csi}	Weighting factor for CSI	1
λ_{buck}	Weighting factor for Buck	4

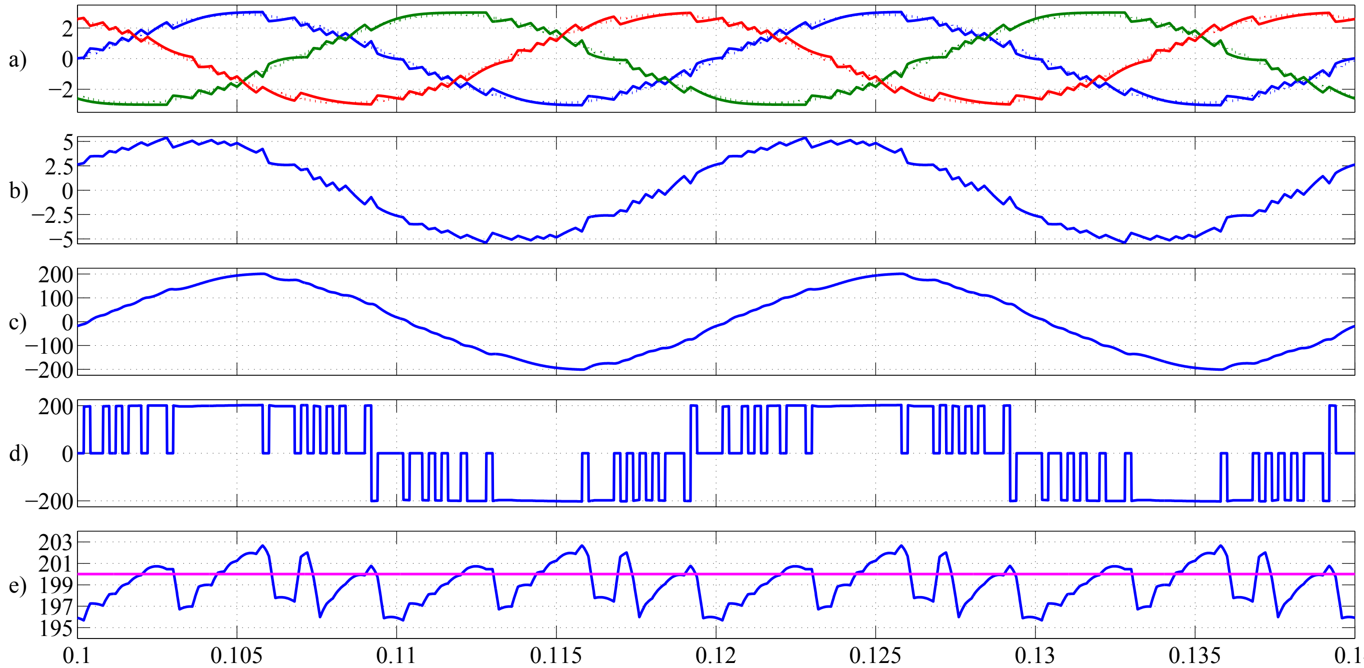

Fig. 2. Simulation results under nominal conditions; a) capacitor voltage measurements and references [kV], b) line-to-line output voltage v_{ab} [kV], c) output current i_a [A], d) inverter output current of phase a i_{inv_a} [A], e) inductor current i_{dc} [A]

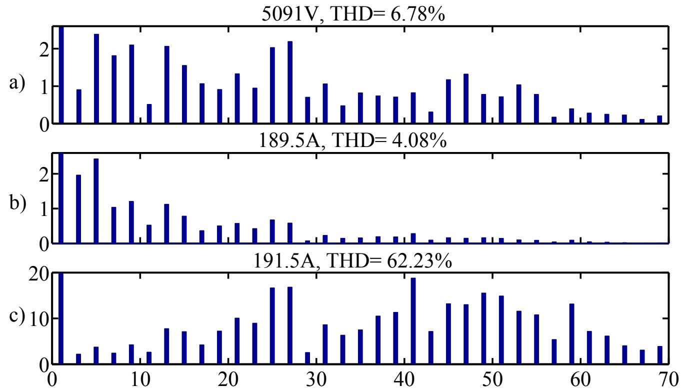

Fig. 3. Spectrum of waveform versus harmonic order; a) line-to-line output voltage v_{ab} [V], b) output current i_a [A], c) inverter output current i_{inv_a} [A]

A. Nominal conditions

The simulated waveforms of the inverter under nominal conditions are shown in Fig. 2. An acceptable tracking of the output voltage to its reference is shown in Fig. 2a. This is achieved with a low switching frequency as depicted in Fig. 2d. Line to line voltage v_{ab} is presented in Fig. 2b. The output current i_a, Fig. 2c, shows an almost sinusoidal waveform. In Fig. 2e, the output current of the buck converter is shown and it can be seen that it tracks the reference with a ripple as low as $\pm$ 4A. Under these conditions an average switching frequency of about 600Hz is obtained for the CSI while the buck converter switch S_7 presents an average switching frequency of 350Hz. As shown in Fig. 3, the i_{inv_a} THD is 62%, while the distortion of i_a is reduced to almost 4% due to the filter capacitor and the line to line voltage is less than 7%.

B. Output Voltage Step

A step of the reference voltages from 2.9kV to 1.7kV is applied at time 0.16s and results are shown in Fig. 4. The controller tracks almost immediately the reference change while the i_{dc} current remains around its reference. In this case, the THD of v_{ab} and i_a increases to 10% and 5% respectively with an increment in the average switching frequency of the inverter up to 800Hz. The average switching frequency of the buck converter also increases to 600Hz. The ripple of i_{dc} remains practically constant as shown in Fig. 4e. The switching frequency increases because the switches of the CSI jump to the zero state more frequently in order to achieve a lower output current caused by the change in the reference voltages. As expected, the controller behaves robustly tracking the references.

C. Current Input Step

While keeping the output voltage reference at 1.7kV, a reduction of 49% is applied to the current reference of the buck converter. The results can be seen on Fig. 5. The current i_{dc} settles in less than 12ms. After the current settles, the output voltage waveforms $v_{a,b,c}$ present the same shape as in Sub. IV-A with the same voltage THD, current THD and average switching frequency of the inverter. The only observed change is the average switching frequency of the buck converter that increases up to 800Hz in this case. This results also shows the robustness of the proposed controller.

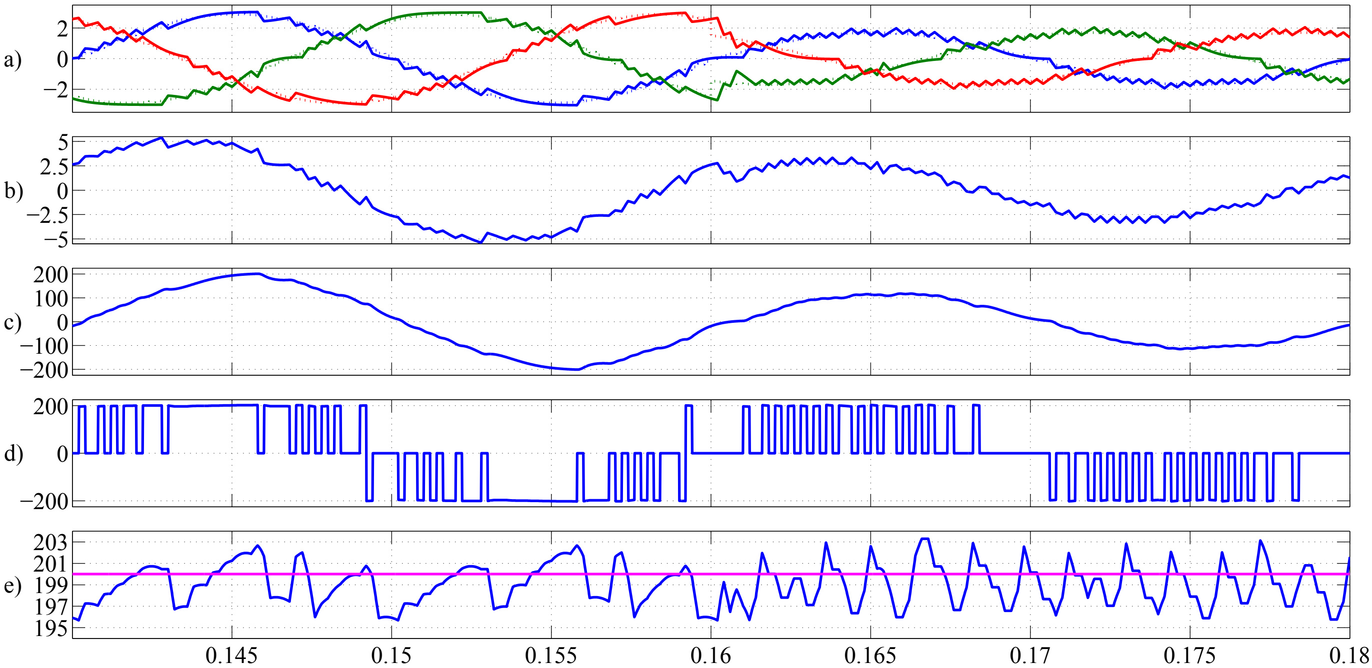

Fig. 4. Simulation results for predictive control of the system with a step change in voltage references; a) capacitor voltage measurements and references [kV], b) line-to-line output voltage v_{ab} [kV], c) output current i_a [A], d) inverter output current of phase a i_{inv_a} [A], e) inductor current i_{dc} [A]

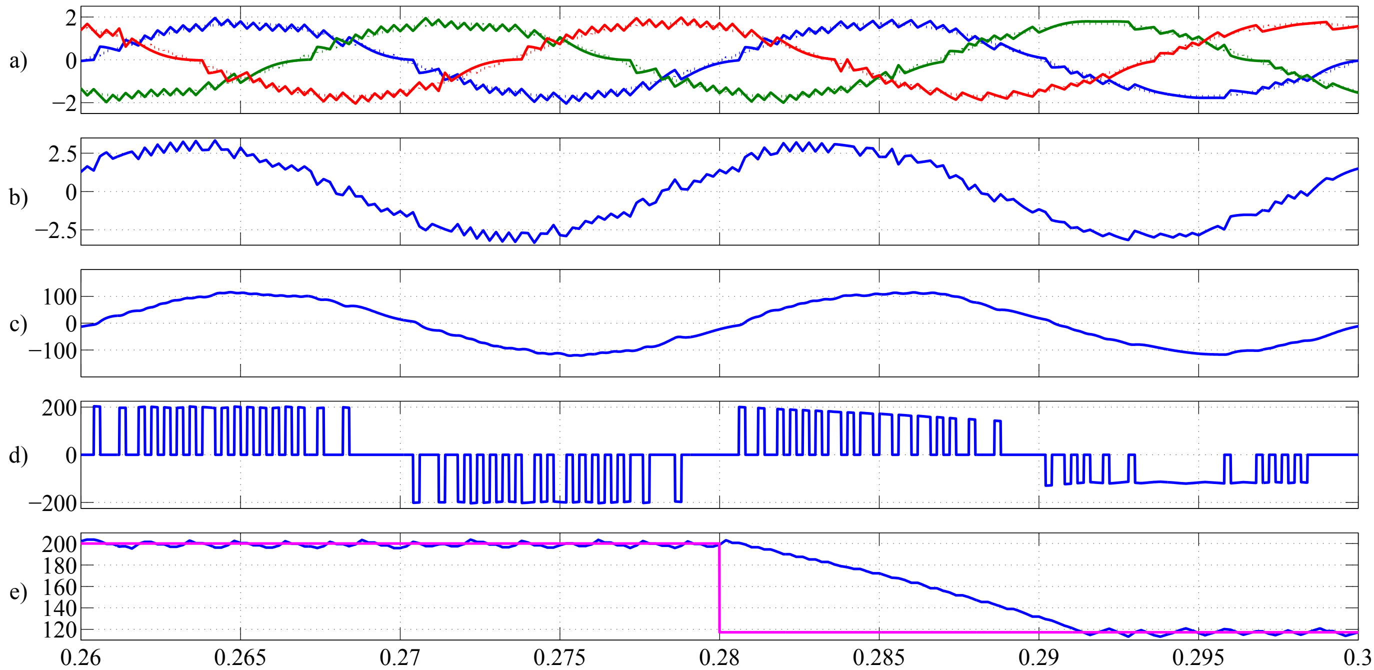

Fig. 5. Simulation results under a step change in current reference; a) capacitor voltage measurements and references [kV], b) line-to-line output voltage v_{ab} [kV], c) output current i_a [A], d) inverter output current of phase a i_{inv_a} [A], e) inductor current i_{dc} [A]

V. Conclusion

The predictive capacitor voltage control strategy of a current source inverter and its current source, which is implemented using a buck converter, has been presented. The discrete time model of the plant has been described and used to predict the best suited switching state that must be applied at the next sampling period. The inclusion of the switching state of the buck converter within the controller allows the use of a non constant power source because it also controls the current fed to the CSI. Using a simple but effective cost function, the algorithm shows a good reference tracking and a reduction of 40% on the switching frequency of the inverter in comparison with the SPWM modulation under the same load and input conditions. In addition, it also provides a low switching frequency of the buck converter. Thus, reducing the switching losses and increasing the efficiency of the whole system. The proposed controller shows a robust behaviour under abrupt changes on both of its references.

REFERENCES

[1] H. Gao, S. Das, B. Wu, M. Pande, and D. Xu, "A space vector modulation based direct torque control scheme for a current source inverter fed induction motor drive," in *Industrial Electronics Society, IECON 2015 - 41st Annual Conference of the IEEE*, Nov 2015, pp. 001 307–001 312.

[2] E. S. Najmi and A. Ajami, "Modular symmetric and asymmetric reduced count switch multilevel current source inverter," *IET Power Electronics*, vol. 9, no. 1, pp. 51–61, 2016.

[3] Q. Wei, B. Wu, D. Xu, and N. Zargari, "A medium frequency transformer-based wind energy conversion system used for current source converter based offshore wind farm," *IEEE Transactions on Power Electronics*, vol. PP, no. 99, pp. 1–1, 2016.

[4] P. Cossutta, M. P. Aguirre, A. Cao, S. Raffo, and M. I. Valla, "Single-stage fuel cell to grid interface with multilevel current-source inverters," *IEEE Transactions on Industrial Electronics*, vol. 62, no. 8, pp. 5256–5264, Aug 2015.

[5] M. Mao, Y. Zheng, L. Chang, and H. Xu, "A single-stage high gain current source inverter for grid-connected photovoltaic system," in *2015 9th International Conference on Power Electronics and ECCE Asia (ICPE-ECCE Asia)*, June 2015, pp. 1902–1907.

[6] S. Jayalath and M. Hanif, "Controller tuning for a single phase grid-connected current source inverter," in *Future Energy Electronics Conference (IFEEC), 2015 IEEE 2nd International*, Nov 2015, pp. 1–6.

[7] N. Mittal, B. Singh, S. Singh, R. Dixit, and D. Kumar, "Multilevel inverters: A literature survey on topologies and control strategies," in *Power, Control and Embedded Systems (ICPCES), 2012 2nd International Conference on*, Dec 2012, pp. 1–11.

[8] S. Anand, S. K. Gundlapalli, and B. G. Fernandes, "Transformer-less grid feeding current source inverter for solar photovoltaic system," *IEEE Transactions on Industrial Electronics*, vol. 61, no. 10, pp. 5334–5344, Oct 2014.

[9] S. Kouro, M. A. Perez, J. Rodriguez, A. M. Llor, and H. A. Young, "Model predictive control: Mpc's role in the evolution of power electronics," *IEEE Industrial Electronics Magazine*, vol. 9, no. 4, pp. 8–21, Dec 2015.

[10] A. Formentini, A. Trentin, M. Marchesoni, P. Zanchetta, and P. Wheeler, "Speed finite control set model predictive control of a pmsm fed by matrix converter," *IEEE Transactions on Industrial Electronics*, vol. 62, no. 11, pp. 6786–6796, Nov 2015.

[11] M. Vijayagopal, L. Empringham, L. de Lillo, L. Tarisciotti, P. Zanchetta, and P. Wheeler, "Current control and reactive power minimization of a direct matrix converter induction motor drive with modulated model predictive control," in *2015 IEEE International Symposium on Predictive Control of Electrical Drives and Power Electronics (PRECEDE)*, Oct 2015, pp. 103–108.

[12] Z. Zhang, H. Fang, and R. Kennel, "Novel ripple reduced direct model predictive control of three-level npc active front end with reduced computational effort," in *2015 IEEE International Symposium on Predictive Control of Electrical Drives and Power Electronics (PRECEDE)*, Oct 2015, pp. 32–37.

[13] M. Parvez, S. Mekhilef, N. M. L. Tan, and H. Akagi, "An improved active-front-end rectifier using model predictive control," in *Applied Power Electronics Conference and Exposition (APEC), 2015 IEEE*, March 2015, pp. 122–127.

[14] L. Ben-Brahim, A. Gastli, M. Trabelsi, K. Ghazi, M. Houchati, and H. Abu-Rub, "Modular multilevel converter circulating current reduction using model predictive control," *IEEE Transactions on Industrial Electronics*, vol. PP, no. 99, pp. 1–1, 2016.

[15] O. Abdel-Rahim and H. Funato, "Five-level multilevel power conditioning system for grid-tie photovoltaic applications with novel model predictive control," in *Future Energy Electronics Conference (IFEEC), 2015 IEEE 2nd International*, Nov 2015, pp. 1–6.

[16] J. Rodriguez, S. Bernet, P. K. Steimer, and I. E. Lizama, "A survey on neutral-point-clamped inverters," *IEEE Transactions on Industrial Electronics*, vol. 57, no. 7, pp. 2219–2230, July 2010.

[17] C. Du, J. Zhou, and Y. Ma, "Predictive current control of a current-source inverter with active damping method," in *Energy Conversion Congress and Exposition (ECCE), 2015 IEEE*, Sept 2015, pp. 1100–1104.

[18] D. K. Choi and K. B. Lee, "Dynamic performance improvement of ac/dc converter using model predictive direct power control with finite control set," *IEEE Transactions on Industrial Electronics*, vol. 62, no. 2, pp. 757–767, Feb 2015.

[19] S. Vazquez, J. I. Leon, L. G. Franquelo, J. Rodriguez, H. A. Young, A. Marquez, and P. Zanchetta, "Model predictive control: A review of its applications in power electronics," *IEEE Industrial Electronics Magazine*, vol. 8, no. 1, pp. 16–31, March 2014.

[20] M. Aguirre, L. Calviño, and M. Valla, "Multilevel current-source inverter with fpga control," *Industrial Electronics, IEEE Transactions on*, vol. 60, no. 1, pp. 3 –10, jan. 2013.

[21] M. Rivera, S. Kouro, J. Rodriguez, B. Wu, and J. Espinoza, "Predictive control of a current source converter operating with low switching frequency," in *IECON 2012 - 38th Annual Conference on IEEE Industrial Electronics Society*, Oct 2012, pp. 674–679.

[22] O. Kukrer, "Discrete-time current control of voltage-fed three-phase pwm inverters," *Power Electronics, IEEE Transactions on*, vol. 11, no. 2, pp. 260–269, Mar 1996.